THE ASTROPHYSICAL JOURNAL, 243:589–596, 1981 January 15

VLBI OBSERVATIONS OF SS 433 AT 3.6 AND 13 CENTIMETERS

R. C. WALKER, A. C. S. READHEAD, AND G. A. SEIELSTAD
California Institute of Technology

R. A. PRESTON, A. E. NIELL, AND G. M. RESCH
Jet Propulsion Laboratory

P. C. CRANE AND D. B. SHAFFER
National Radio Astronomy Observatory, Green Bank

B. J. GELDZAHLER
Max-Planck-Institut für Radioastronomie

S. G. NEFF
National Radio Astronomy Observatory, Charlottesville

I. I. SHAPIRO
Massachusetts Institute of Technology Cambridge,

D. L. JAUNCEY
Division of Radiophysics, C.S.I.R.O., Sidney, Australia

AND

G. D. NICOLSON
CSIR, Johannesburg, South Africa

Received 1980 June 2; accepted 1980 August 6

ABSTRACT

SS 433 was detected and partially resolved at 2290 MHz on baselines with fringe spacings of 1″.4, 0″.1, and 0″.003. It was also detected at 8420 MHz on a baseline with a fringe spacing of 0″.009. Simple models of the source, consistent with the limited data, have elongated structures greater than 0″.1 in size with position angles in 1979 May that were within about 10° of the position angle of the apparent bulges of the supernova remnant W50. The data also imply that the source contains a core less than 0″.002 in size with a brightness temperature greater than 10^9 K. The bright core and aligned structures that seem to be present in SS 433 and W50 resemble the structures seen in powerful extragalactic radio sources which are many orders of magnitude larger.

Subject headings: nebulae: supernova remnants — radio sources: general — stars: emission-line — stars: individual — stars: radio radiation

I. INTRODUCTION

SS 433 is an object distinguished by the presence of optical emission lines which exhibit velocity shifts of thousands of km s^{-1} on time scales of days or less (Margon *et al.* 1979*b*). Margon *et al.* (1979*a*) and Liebert *et al.* (1980) have established that the moving lines belong to two systems which shift, with opposite phase, over the velocity range −35,000 to +50,000 km s^{-1}, with a 164 day period. Fabian and Rees (1979) and Milgrom (1979) have suggested that the moving lines arise in two oppositely directed, relativistic jets.

The optical position of SS 433 coincides with that of a compact radio source in the center of the supernova remnant W50 (Geldzahler, Pauls, and Salter 1980; Kaplan *et al.* 1980). Several authors (Spencer 1979; Gilmore and Seaquist 1980; Hjellming, Johnston, and Miley 1979) have shown that the radio source has arc-second scale structure that is aligned with pronounced bulges in the supernova remnant. In this paper, we report the results of VLBI observations which are consistent with the presence of a compact core and extended components about 0″.1 and 2″ in size. The extended components are roughly aligned with the bulges in W50. The alignment between the small-scale (<0″.1) and large-scale (2°) features is probably not fortuitous. Similar alignment between nuclear cores and outer lobes is observed in many extragalactic radio sources (Readhead *et al.* 1978, and references cited therein). Recent theories of the formation of extragalactic radio sources also involve relativistic jets (see Blandford and Konigl 1979).

II. THE OBSERVATIONS

Three sets of VLBI observations of SS 433 were made in 1979 May. A summary of the telescope systems used is given in Table 1. On May 12 a complete

TABLE 1

SS 433 VLBI: STATION PARAMETERS

Location	Abbrev.	Diameter (m)	Frequency Standard	Radio Frequency[a]	T_s[b] (K)	Experiment[c]
Hartebeesthoek, South Africa	HBK	26	Rubidium	S	24	B
Madrid, Spain......	DSS63	64	Maser	S	22	B
				X	24	B
Haystack, MA	HSTK	37	Maser	X	110	B
Green Bank, WV ...	NRAO	43	Maser	X	59	B
Goldstone, CA	DSS13	26	Maser	S	26	A, B, C
Goldstone, CA	DSS14	64	Maser	S	19	B
Owens Valley, CA	OVRO	40	Rubidium	S	140	A, C
				X	300	B
Tidbinbilla, Australia	DSS43	64	Cesium	S	19	C

[a] S = 2290 MHz, X = 8420 MHz.
[b] At zenith.
[c] A, 1979 May 12; B, 1979 May 18; C, 1979, 1979 May 27.

set of observations was obtained on the DSS13-OVRO baseline at 2290 MHz. The second set of observations, made on May 18, involved eight VLBI stations at 2290 MHz and/or 8420 MHz (see Table 1). In addition, flux density measurements were made on the Very Large Array (VLA) of the National Radio Astronomy Observatory. Unfortunately, the observations at DSS43 failed during the second observing session, so a third set of observations from California to Australia was made on May 27.

All observations were made with Mark II VLBI recording terminals (Clark 1973) and were processed on the CIT/JPL processor. The data were calibrated in the manner described by Cohen *et al.* (1975) using system gain factors determined from observations of calibration sources and system temperatures measured hourly during the observations. At 2290 MHz, the gains of all telescopes were assumed to be independent of pointing direction while at 8420 MHz, the data did not warrant the use of anything more precise than nominal zenith gains. The *b*-factor, a correction factor applied to account for amplitude losses inherent in the VLBI system (Cohen *et al.* 1975), was assumed to be 2.5 for all baselines.

III. RESULTS

The results from the observations are presented in Table 2 and in Figures 1 and 2. Failures at some

TABLE 2

SS 433 VLBI: SUMMARY OF RESULTS

Day (1979)	Frequency (MHz)	Baseline	Correlated Flux Density (Jy)	Fringe Spacing (0".001)	P.A. (Deg)
May 12 ...	2290	DSS13–OVRO	0.22–0.38	100 to 130	−22 to 45[a]
May 18 ...	2290	HBK–DSS63	< 0.03	3.6	17
May 18 ...	2290	HBK–DSS13	< 0.07	2.1	58
May 18 ...	2290	DSS63–DSS14	0.02–0.04	3.3	94[a]
May 18 ...	2290	DSS63–DSS13	< 0.03	3.3	94
May 18 ...	2290	DSS13–DSS14	0.72–0.90	1200 to 1500	−9 to 40[a]
May 27 ...	2290	DSS13–OVRO	0.20 ± 0.04	100.	46
May 27 ...	2290	OVRO–DSS43	< 0.03	2.5	−45
May 27 ...	2290	DSS13–DSS43	< 0.02	2.5	−45
May 18 ...	8420	DSS63–HSTK	< 0.045	1.5	96
May 18 ...	8420	DSS63–NRAO	< 0.03	1.3	94
May 18 ...	8420	DSS63–OVRO	< 0.13	0.9	92
May 18 ...	8420	HSTK–NRAO	0.11 ± 0.03	9.	−66
May 18 ...	8420	HSTK–OVRO	< 0.54	2.0	96
May 18 ...	8420	NRAO–OVRO	< 0.37	2.5	92

[a] See Figs. 1 and 2 for details.

1981ApJ...243..589W

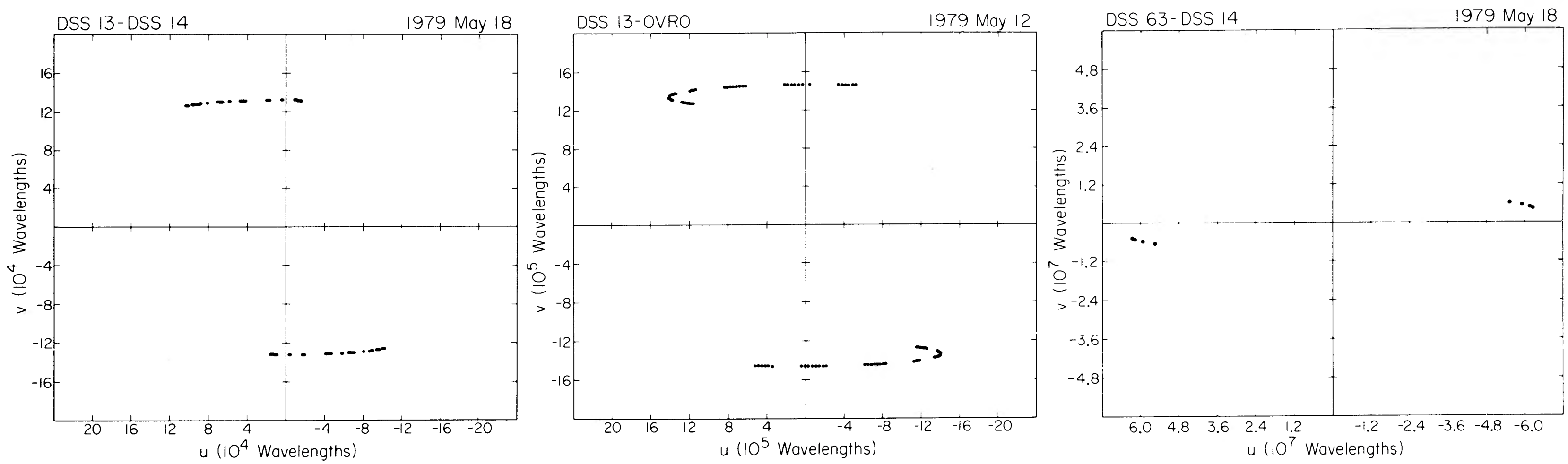

FIG. 1.—The *u-v* tracks corresponding to the data in Fig. 2. Note the different orders of magnitude in the scales.

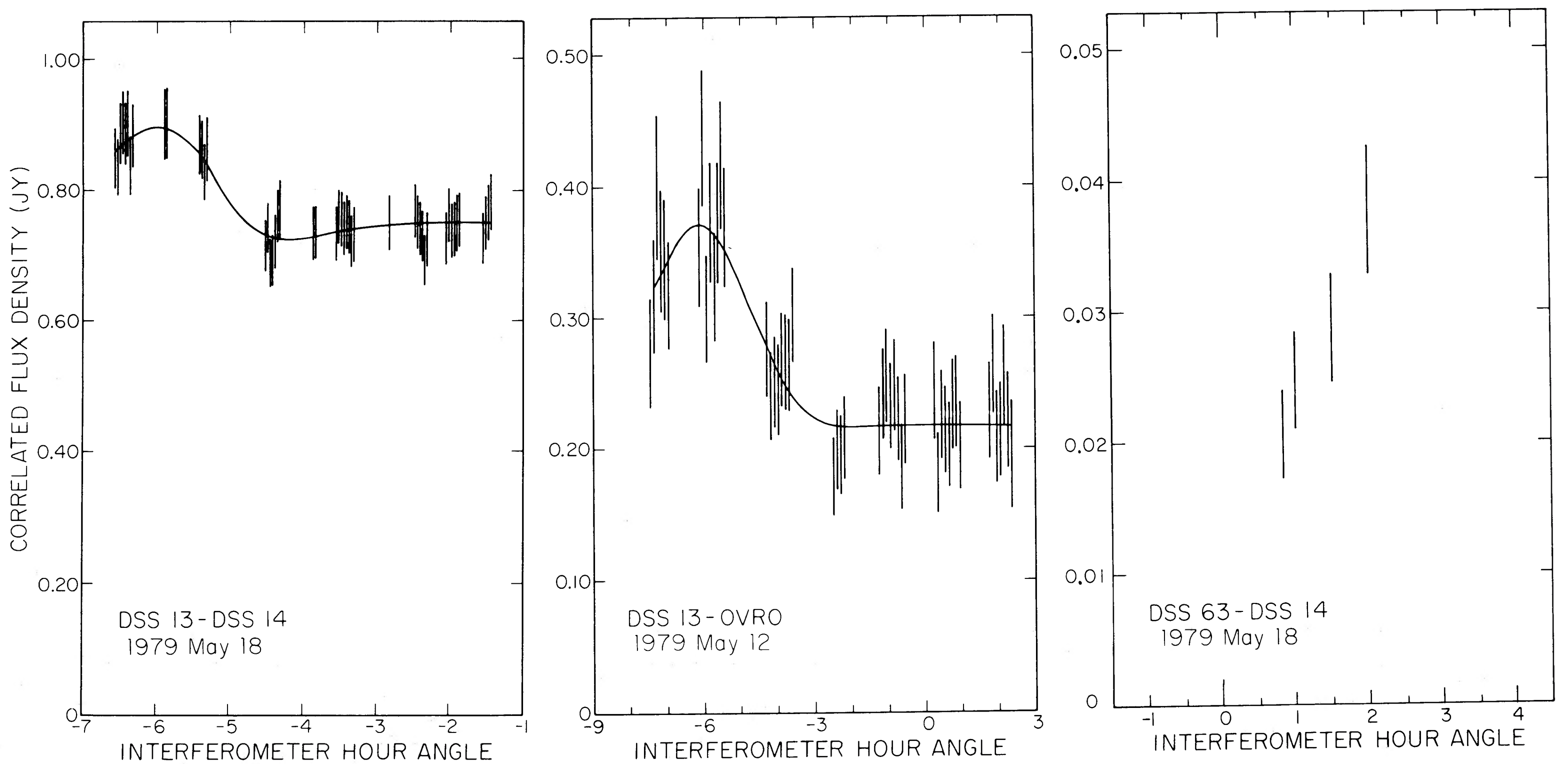

FIG. 2.—Correlated flux density vs. interferometer hour angle for the DSS13–DSS14, DSS13–OVRO, and DSS63–DSS14 baselines. The solid lines show the predictions of the models in Table 4.

stations rendered the data on some baselines useless. Table 2 shows results from only those baselines and frequencies for which fringes of the expected amplitude were obtained from observations of strong sources (e.g., P2134+004, 3C 345, 3C 273). For most of the baselines, the *u-v* coverage was minimal due to the low declination (5°) of SS 433, so only the mean fringe spacing and baseline position angle are given. SS 433 was detected on the DSS13–DSS14, DSS13–OVRO, and DSS14–DSS63 baselines at 2290 MHz. The *u-v* tracks and data for the DSS13–OVRO baseline on May 12 and for the other two baselines on May 18 are shown in Figures 1 and 2. On May 27 the *u-v* coverage for the DSS13–OVRO baseline was very limited because the first few hours of observing were missed. The data that were obtained on that day are not shown because the correlated flux densities were constant to within their estimated uncertainties and were consistent with the correlated flux densities obtained on May 12. At 8420 MHz, the source was detected in three consecutive 1 hour coherent integrations on the HSTK–NRAO baseline. The correlated flux densities were surely reduced by coherence loss during these unusually long integrations. A correction factor of 1.2, determined by comparison of a one hour integration with short integrations on 3C 273 on the same baseline on the same day, was applied to the data. The large uncertainty in the correlated flux density reflects the uncertainty in this correction. For most of the baselines in Table 2, only upper limits to the correlated flux density are available. Each upper limit represents about 3.5 times the rms noise for the longest reasonable coherent integration time (typically 15 minutes) for the baseline as determined by a fringe amplitude loss of 20–50% in observations of strong sources.

The available information on the total flux density of SS 433 on May 18 and May 27 is presented in Table 3. The total flux density given for 8420 MHz is extrapolated from the flux densities at the other frequencies assuming a power law spectrum with a spectral index of $\alpha = -0.5$. No flux density measurements are available for May 12. Continuous monitoring data at DSS43 on May 18 and May 27 showed no short term variability above the estimated 2% uncertainty of the measurements during approximately 6 hours of observations at that telescope on each day (for details of the flux density measurement methods at DSS43, see Batty *et al.* 1980). Therefore changes in correlated flux density during each day are assumed to be due to source structure rather than to variations in the total flux density.

TABLE 3

SS 433 Flux Density

Frequency (MHz)	Date (1979)	Telescope	Flux Density (Jy)
1414........	May 18	VLA	1.2 ± 0.2
2290........	May 18	DSS43	0.98 ± 0.02
3240........	May 18	NRAO 91 m	0.82 ± 0.08[a]
4995........	May 18	VLA	0.65 ± 0.1
8420........	May 18	Extrapolated	0.50 ± 0.1
2290........	May 27	DSS43	0.83 ± 0.02

[a] Heeschen and Hammond 1980.

The VLBI data are not sufficiently extensive to allow a map or even a detailed model to be made of SS 433. However, the variations in the correlated flux density as a function of hour angle on the DSS13–DSS14 and DSS13–OVRO baselines give an indication of the flux density and position angles of structure in the source on scales similar to the fringe spacings for those baselines. Note that separate models are required for the two baselines because the fringe spacings differ by an order of magnitude. The data from both baselines show peaks when the projected baselines are nearly north-south. At other hour angles, the correlated flux density is lower and nearly constant. Such data can be reproduced by a wide variety of models that are extended in roughly the east-west direction. The data from each baseline can be matched to within the estimated errors by models ranging from double point sources to core-halo configurations with elongated halos. An intermediate model consisting of a point source and an offset, elongated Gaussian matches the data from each baseline more satisfactorily than either of the cases mentioned above. The parameters of a model of this type for each baseline are presented in Table 4, and the predictions of the models are shown as solid lines in Figure 2. For each of the models, the major-axis position angle was held equal to the offset position angle in order to maintain a well-defined source position angle and reduce the number of degrees of freedom.

The parameters of the models in Table 4 are not tightly constrained. Large variations in any one parameter can be offset by variations in the other parameters to maintain a good fit to the data. For each parameter, the approximate range of values over which models consistent with the data could be found was determined by attempting to fit the data while holding the parameter fixed at several different values. A value was considered within the allowed range if the predictions of the model fell within the error bars of the data and the total flux density of the model did not exceed the measured total flux density of the source. The ranges derived from these tests are shown in Table 4. No attempt was made to try models consisting of components other than one point source and one Gaussian. Note that we did not obtain any useful phase information, so there is a 180° ambiguity in the offset position angles.

The data from the DSS63–DSS14 baseline show that there are at least 30 mJy in a compact core about 0.″002

TABLE 4

MODELS OF SS 433

PARAMETER	DSS13–DSS14 1979 MAY 18 Model Value[a]	Range of Acceptable Values	DSS13–OVRO 1979 MAY 12 Model Value[a]	Range of Acceptable Values
Point Source at Origin:				
Flux density (Jy)	0.75	0.74–0.80	0.24	0.21–0.29
Offset Gaussian:				
Flux Density (Jy)	0.17	0.12–0.24	0.13	0.08–0.8
Offset (arcsec)	1.5	0.0–2.5	0.064	0.0–0.095[b]
Major axis (arsec–FWHM)	2.6	1.3–4.5[c]	0.10	0.0–0.25[b]
Axial ratio	0.1	0.0–0.2	0.1	0.0–0.7
Position angle of offset and major axis (degrees) (constrained to be equal)	90	87–95[d]	92	85–105

[a]Values used for models plotted in Fig. 2.

[b]The source is elongated, so the offset and the major axis cannot both be zero in an acceptable model.

[c]A double point source (major axis = 0.0) gives predictions barely within the error bars but shows a pronounced sinusoidal structure not seen in the data.

[d]Models with position angles up to 110° give predictions within the error bars but do not show the peak apparent in the correlated flux densities at early hour angles.

in size. There are not sufficient data to provide any information on the structure of the core. The brightness temperature of the core is at least 10^9 K.

There is very little information about the source at 8420 MHz. A detection was obtained on only one baseline (HSTK-NRAO) and yielded a ratio of correlated flux density to total flux density of 0.2 ± 0.1 with a fringe spacing of 0".009.

IV. DISCUSSION

Structure has been observed in SS 433 on scales of 0".1 and 2" at 2290 MHz (this paper), 1" at 408 MHz (Spencer 1979), and 0".2 and greater at 1.5 and 4.9 GHz (Gilmore and Seaquist 1980; Hjellming *et al.* 1979). Each of these observations shows that the source is elongated with a position angle between 90° and 110°, although Gilmore and Seaquist (1980) find complicated structure at 1.5 GHz. On scales less than 0".1, only detections and upper limits have been reported (this paper; Schilizzi *et al.* 1979; Geldzahler, Downes, and Shaffer 1980). These observations show that SS 433 is likely to have structure on all scales between 0".001 and 2". However, more information on the structure on scales less than 0".1 will be difficult to obtain due to the small flux density in the compact components. The large-scale structure of W50 shows a fairly circular shell source with pronounced bulges on either side, symmetric about a position angle of $98° \pm 5°$ (cf. Geldzahler, Pauls, and Salter 1980) which is consistent with the position angles derived above for SS 433. This alignment is circumstantial evidence for the physical association of SS 433 with W50 and against the possibility that the bulges are foreground or background objects unrelated to W50.

The kinematic model of Abell and Margon (1979) requires that the optical jets rotate so that they move on the surface of a cone of half-angle 20° (Margon, private communication). If the jets are responsible for the bulges in W50, it is reasonable to assume that the axis of symmetry of this cone is aligned with the radio structure along the 98° position angle of the supernova remnant. The size of the 0".1 elongated radio feature in our model for the data from the DSS13–OVRO baseline is about 5×10^{15} cm (if the distance to SS 433 is 3.5 kpc), or somewhat larger than the estimated size of the optical emission region ($10^{12}-10^{15}$ cm; cf. Begelman *et al.* 1980). It is important to determine whether this radio component is rotating with the optical jets. Such rotation cannot be ruled out by the present observations. The Abell-Margon model predicts that the projected angle between the optical jets and the axis of the cone on May 12 was 9° and increasing. The May 12 data are more consistent with a position angles of $98° - 9°$ than with $98° + 9°$. Thus, if this radio component is rotating with the optical jets, its position angle was probably decreasing in the quarter-cycle which fell between May 1 and June 10. The data are also consistent with a nonrotating component which is aligned with the supernova remnant. If the 0".1 component is rotating, its apparent alignment with the 2″6 component in the model for the data from the DSS13–DSS14 baseline is probably fortuitous since Spencer (1979) has shown that the radio structure on a 1″0 scale does not rotate with the optical jets. Further observations on the DSS13–OVRO baseline, at suitably chosen phases of the rotational motion, are planned to determine whether or not the 0″1 extended feature is rotating. Note that our data allow only crude limits to be placed on the widths of the elongated structures, so it is possible that the extended components are fairly broad, filling the 40° sector of the rotational cone.

The relative strengths of the observed optical emission lines imply that the temperature of the gas responsible for the high velocity lines is probably not much greater than 10^4 K (Begelman *et al.* 1980; Fabian and Rees 1979). Katz (1980) has suggested that thermal processes may be accelerating the material in the beams. The radio properties of the source show that relativistic gas must also be present throughout most of SS 433. The high brightness temperature of the core shows that relativistic gas is present in the innner 10^{14} cm, while the nonthermal integrated spectrum shows that it is also present in the larger regions which are responsible for the bulk of the radio emission.

The most striking fact to emerge from the high resolution observations is the apparent alignment between the small-scale and large-scale features. If the bulges in W50 are caused by material beamed from SS 433, then we would have a situation very similar to that thought to exist in many extragalactic radio sources. In fact, the whole object resembles the superposition of a supernova remnant and an extragalactic triple source with two outer lobes and a central core. The mass of SS 433 is probably nine orders of magnitude smaller than that of a typical radio galaxy. It would be very interesting if the same mechanism were responsible for the relativistic jets which have been postulated to exist in both types of object.

We thank Arieh Konigl for useful discussion concerning position angles and the dynamical model, P. F. MacDoran for calling attention to the opportunity of 1979 May 12, the personnel of JPL's Project ARIES for volunteering their time for the observations of May 12, and R. L. Brown for cooperation with the VLA observations. The National Radio Astronomy Observatory is operated by the Associated Universities, Incorporated, under contract to the National Science Foundation. The Haystack Observatory is operated by the Northeast Radio Observatory Corporation with support from the National Science Foundation. Astronomy at the Owens Valley Radio Observatory is supported by the National Science Foundation via grant AST 7700247. This paper presents results from one phase of research carried out at the Jet Propulsion Laboratory, California Institute of Technology, under contract NAS 7-100, sponsored by the National Aeronautics and Space Administration.

REFERENCES

Abell, G. O., and Margon, B. 1979, *Nature*, **279**, 701.
Batty, M. J., Jauncey, D. L., Rayner, P. T., and Gulkis, S. 1980, preprint.
Begelman, M. C., Sarazin, C. L., Hatchett, S. P., McKee, C. F., and Arons, J. 1980, *Ap. J.*, **238**, 722.
Blandford, R. D., and Konigl, A. 1979, *Ap. J.*, **232**, 34.
Clark, B. G. 1973, *Proc. IEEE*, **61**, 1242.
Cohen, M. H., *et al.* 1975, *Ap. J.*, **201**, 249.
Fabian, A. C., and Rees, M. J. 1979, *M.N.R.A.S.*, **187**, 13p.
Geldzahler, B. J., Downes, A. J. B., and Shaffer, D. B. 1980, preprint.
Geldzahler, B. J., Pauls, T., and Salter, C. J. 1980, *Astr. Ap.*, **84**, 237.
Gilmore, W. S., and Seaquist, E. R. 1980, preprint.
Heeschen, D. S., and Hammond, S. E. 1980, *Ap. J.* (*Letters*), **235**, L129.
Hjellming, R. M., Johnston, K. J., and Miley, G. K. 1979, *Bull. AAS*, **11**, 673.
Kaplan, G. H., Kallarkal, V. V., Harrington, R. S., Johnston, K. J., and Spencer, J. H. 1980, *A.J.*, **85**, 64.
Katz, J. I. 1980, *Ap. J.* (*Letters*), **236**, L127.
Liebert, J., Angel, J. R. P., Hege, E. K., Martin, P. G., and Blair, W. 1979, *Nature*, **279**, 384.
Margon, B., Ford, H. C., Grandi, S. A., and Stone, R. P. S. 1979*a*, *Ap. J.* (*Letters*), **233**, L63.
Margon, B., Ford, H. C., Katz, J. I., Kwitter, K. B., Ulrich, R. K., Stone, R. P. S., and Klemola, A. 1979*b*, *Ap. J.* (*Letters*), **230**, L41.
Milgrom, M. 1979, *Astr. Ap.*, **76**, L3.
Readhead, A. C. S., Cohen, M. H., Pearson, T. J., and Wilkinson, P. N. 1978, *Nature*, **276**, 768.
Schilizzi, R. T., Norman, C. A., van Breugel, W., and Hummel, E. 1979, *Astr. Ap.*, **79**, L26.
Spencer, R. 1979, *Nature*, **282**, 483.

P. C. Crane: National Radio Astronomy Observatory, P.O. Box 2, Green Bank, WV 24944

B. J. Geldzahler and I. I. Shapiro: Dept. of Earth and Planetary Sciences, Room 54-622, Massachusetts Institute of Technology, Cambridge, MA 02139

D. L. Jauncey: Division of Radiophysics, c/o Soils, P.O. Box 639, Canberra City 2601, ACT, Australia

S. G. Neff and R. C. Walker: National Radio Astronomy Observatory, Edgemont Road, Charlottesville, VA 22901

G. D. NICOLSON: Radio Astronomy Observatory, NITR, P.O. Box 3718, Johannesburg 2000, South Africa

A. E. NIELL and G. M. RESCH: Jet Propulsion Laboratory 264-765, 4800 Oak Grove Drive, Pasadena, CA 91103

R. A. PRESTON: Jet Propulsion Laboratory 264-720, 4800 Oak Grove Drive, Pasadena, CA 91103

A. C. S. READHEAD: Caltech 102-24, Pasadena, CA 91125

G. A. SEIELSTAD: Owens Valley Radio Observatory, P.O. Box 387, Big Pine, CA 93513

D. B. SHAFFER: NASA–Goddard Space Flight Center, Code 945, Greenbelt, MD 20771